Mechanism of Liquefaction-Induced Large Settlements of Buildings

ZAHEER AHMED ALMANI*, KAMRAN ANSARI*, AND ASHFAQUE AHMED MEMON*

RECEIVED ON 08.02.2012 ACCEPTED ON 21.06.2012

ABSTRACT

In this paper, mechanism of liquefaction-related large settlements of the soil-structure system during the earthquake was studied using numerical modelling. The isolated shallow strip plane strain footing pad, supporting a typical simple frame structure, was founded on the ground at the shallow depth from the level ground surface. This system was modelled as plane-strain using the FLAC (Fast Lagrangian Analysis of continua) 2D dynamic modelling and analysis code. This case focuses on the basic mechanisms of liquefaction-induced large deformations of the structure during an earthquake and will provide a benchmark model case for comparison with the model case in which jet grouted columns are provided as ground reinforcement. The results showed that large settlements of shallow foundations in punching shear are triggered during cyclic excitation. These large settlements under the structure are driven by load of structure and earthquake excitation. Monotonic shear deformation, lateral shear deformations and volume change of soil are main phenomena under the structure when the pore pressure rises and soil is liquefied in cyclic loading.

Key Words: **Liquefaction, Ground Reinforcement, Numerical Modelling; Settlements, Shalow Foundation.**

1. INTRODUCTION

The buildings on shallow foundations constructed over liquefiable loose or medium dense sand deposits in coastal areas or where water is high, suffer significant damage, disruption of function and considerable replacement expense due to liquefaction-induced settlements and tilting. These large settlements are triggered due to; bearing capacity failure (shear failure) when the soil loses shear stiffness as a result of liquefaction and due to reconsolidation (densification) when pore water is dissipated and volume change of the soil occurs. This type of response of shallow foundations have been reported during earthquakes such as Niigata, Japan, [1], Dagupan City, Philippines, [2], Chi-Chi, Taiwan, [3] and Kocaeli, Turkey, [4-5].

The effective design and construction of liquefaction mitigation techniques requires an improved understanding of the development and results of liquefaction.. Further, the relative importance of key settlement mechanisms could be assessed by applying remediation techniques to limit their respective contributions.

The state-of-the-practice to estimate liquefaction-induced building settlement relies mostly on empirical procedures which estimate post-liquefaction consolidation settlement.

* Assistant Professor, Department of Civil Engineering, Mehran University of Engineering & Technology, Jamshoro.

Mitigation techniques are required when the estimated settlements exceed the building tolerable limits for safety and serviceability. Estimating building settlement based on post-liquefaction empirical procedures considering reconsolidation volumetric strains may neglect the importance of other mechanisms that could damage the buildings. For example, shear or deviatoric deformation within the liquefiable soil under a shallow foundation of building, as well as volumetric strains due to drainage during shaking, can lead to large building movements [6]. These current procedures do not consider these mechanisms of settlements, thus might underestimate the results of liquefaction, the need for ground improvement and the subsequent assessment of the performance of a proposed mitigation scheme.

The effective remediation of the soil liquefaction hazard requires an understanding of the potential hazards of liquefaction on the building performance. If the results of liquefaction are predicted unacceptable, ground reinforcement for liquefaction remediation can be developed to control the fundamental settlement mechanisms.

Numerical modelling is a state-of-the-art versatile tool to understand the fundamental mechanisms of liquefaction and related larger settlements. Therefore in this study, numerical modelling was performed, using FLAC 2D code, to understand the fundamental mechanisms of seismic-induced settlement of buildings with rigid foundations on deposits of liquefiable sand.

Thus, in order to understand the mechanism of liquefaction-related large permanent deformations of the soil-structure system during the earthquake, the isolated shallow strip plane strain footing pad, supporting a typical simple frame structure, founded on the ground at the shallow depth from the level ground surface, was modelled using FLAC 2D.

2. THE CASE EVALUATED

One specific case of shallow foundation supporting the building structure, founded on the level ground with following design parameters was evaluated.

2.1 Shallow Foundation and the Supported Superstructure

A spread isolated single square footing with dimensions of 4x4 m and a thickness of 1 m constructed at a depth of 1m from the natural ground surface, supporting a typical central column with cross-sectional dimensions of 1x 0.5m and the length of 5m, which ultimately supports the superstructure as shown in Fig. 1, was taken.

The simplified superstructure considered for this study consists of four rectangular beams, each with cross-sectional dimensions of 1x 0.5m and a length of 10m. The beams are joined together and are pin-supported on the central column at a right angle. The far ends of all the beams are assumed to be simply supported over the roller supports.

The column and beams are modelled by structural beam elements provided with structural logic in FLAC. The concrete footing pad is represented by grid elements which are represented by the linear elastic constitutive model with elastic properties (shear modulus and bulk modulus) and density of structural concrete. The structural elements have rigid connection with the footing grid, representing the column to be rigidly attached to the

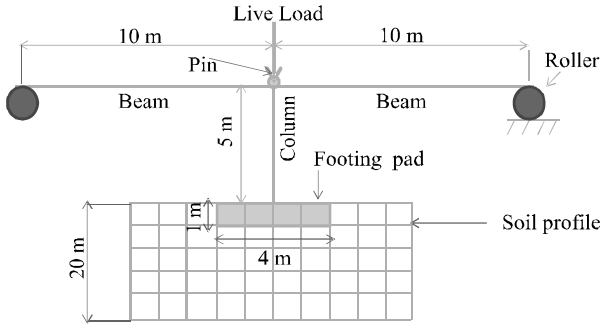

FIG. 1. SUPERSTRUCTURE, COLUMN AND FOOTING FOR ANALYSIS (MESH AND STRUCTURE NOT DRAWN ON SCALE)

footing pad. The beams and columns were assigned masses so that the dead load is properly transferred to the column and then to the footing pad before shaking. During shaking, the superstructure exerts inertial horizontal force on the column and footing pad. As the superstructure beams were supported at their far ends with rollers and the live load was applied at (the pin jointed) top of column, one half of the total live and dead load is transferred to the top of the column and onto the pad. This structure was made with the similar approach as applied in the centrifuge physical tests at Cambridge [7]. The allowable footing bearing pressure for the medium dense sand taken as the foundation soil is in the range of 100-300 kPa as per CP [8]. The lowest footing allowable bearing pressure of 100 kPa in this range for the foundation soil (medium dense sand) was considered in this specific case. The magnitude of the live load on the top of the column was considered in such a way that the bearing pressure on the soil due to both the dead and the live load is 100 kPa. In FLAC 2D plane strain modelling, the structural elements (beams and columns) are assumed to be extended continuously in the transverse direction when in reality they are installed at certain spacing. Therefore, the Young's modulus and the density were divided by the spacing for FLAC 2D input [9]. The properties of the structural members are given in the Table 1.

TABLE 1. PROPERTIES OF STRUCTURAL ELEMENTS

Property	Structural Members (Concrete)	
	Beam	Column
Length (m)	10	5
Cross-Section (mxm)	0.5x1	0.5x1
Area (m^2)	0.5	0.5
Moment of Inertia (m^4)	$4.2x10^{-2}$	$4.2x10^{-2}$
Young's Modulus (MPa)	$25x10^6$	$25x10^6$
Poisson's Ratio	0.15	0.15
Shear Modulus (MPa)	$1x10^7$	$1x10^7$
Bulk Modulus (MPa)	$1.3x10^7$	$1.3x10^7$
Density (kg/m^3)	2400	2400
Permeability (m/sec)	$1x10^{-9}$	$1x10^{-9}$

2.2 The Soil Profile

A two layer soil profile as shown in Fig. 2 was considered. This soil profile consists of 10m thick surface liquefiable medium dense Leighton Buzzard E-Fraction silty sand (at relative density of 40%) with underlying a 10 m thick non liquefiable dense layer of the same sand (at a higher relative density of 80%). Rigid bedrock of infinite extent was considered underlying the dense non liquefiable layer.

The water table was taken at the natural ground surface, thus the whole soil deposit was saturated. Both medium dense and dense sand deposits were assumed to liquefy to different degrees (states). Therefore, both layers were represented by the same liquefaction constitutive model.

2.3 Numerical Modelling Code Selection

There are variety of numerical codes for modelling liquefaction and its remediation. The degree of coupling in these codes vary, some use full coupling (DYNAFLOW and SWANDYNE) while other use partial coupling solutions (FLAC and TARA-3). The selection of a numerical code for modelling liquefaction should depend upon the following criteria:

- o Ability of the code to model liquefaction and its remediation by coupling the dynamic mechanical calculation with flow calculation simultaneously.
- o Ability to include user-defined constitutive models and other changes.

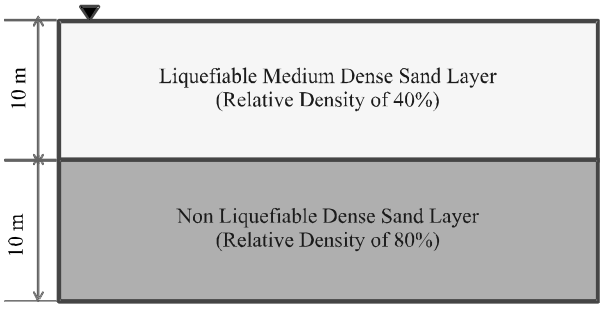

FIG. 2. THE SOIL PROFILE CONSIDERED FOR ANALYSIS

- o Ability to apply free-field boundaries, model structural elements and interfaces
- o Practical viability as accepted by geotechnical engineers and researchers.

The computer codes FLAC 2D Version 6.0 (for Fast Lagrangian Analysis of Continua) as selected for numerical analysis, use an explicit, finite difference formulation for solving geomechanics problems. Material inertia terms are also included in the solution formulation both static and dynamic problems, which require a timestepping procedure. More details regarding codes can be found in the User's Manual [9].

2.4 Coupling of Mechanical Module with Ground Water Flow Module

Liquefaction analysis is a coupled problem in which the mechanical deformation of soil causes the development of pore pressure which results in softening or liquefaction due to which the shear stiffness and strength of soil drops. Due to this softening, further mechanical deformation of soil in undrained condition occurs. This problem can be modelled in the FLAC which is partially-coupled code by coupling the dynamic mechanical module with ground water flow module.

2.5 Basic Soil Properties and Liquefaction Constitutive Model

There is a variety of liquefaction constitutive models ranging from simple empirical models to more theoretical and complex which require larger number of parameters. The use of such complex models with many parameters hardly justify in the face of uncertainties in soil properties and earthquake loading as suggested by Dawson, et.al. as mentioned in FLAC manual [9].

The built-in soil Finn/Byrne model provided with FLAC 2D and 3D for modelling the phenomenon of liquefaction, is based on Mohr-Coulomb elastic-perfectly plastic failure criteria. This soil model can be combined with other built-in hysteric damping models to mimic the behaviour of strain-softening soil [9]. In those damping models, reduction of shear modulus and increase of damping ratio with strain level during dynamic simulation follows modulus reduction curve suggested by Seed, et. al. [10]. The behaviour of liquefiable medium dense and non liquefiable dense layers of Leighton Buzzard E-Fraction sand in this research was represented by the Finn/Byrne liquefaction soil model combined with Hardin-Drnevich hysteretic dynamic damping model as recommended in FLAC Manual [9]. When the soil reached the state of plastic flow, further simulation was continued with only the Finn/Byrne plasticity soil model to avoid unrealistically excessive shear modulus reductions and deformations during plastic flow as suggested in the FLAC dynamic manual [9]. This constitutive model has been successfully applied to model liquefaction and its remediation projects as mentioned in the FLAC manual [9]. This constitutive soil model was calibrated with cyclic constant volume simple shear tests and the model parameters were determined by matching with tests by trial and error. For static analysis, the Mohr-Coulomb soil model was used to represent the response of soil layers.

The basic elastic soil properties such as the small strain shear (G_{max}) and bulk modulus (B) of the soil layers were computed using the Hardin-Drnevich [11] equations suggested for sandy soils.

$$G_{\max} = 100\frac{(3-2)^2}{1+e}(p')^{0.5} \quad (1)$$

Where e is the initial void ratio and p' is confining pressure here, e is the

$$B = \frac{2G_{\max}(1-\nu)}{3(1-2\nu)} \quad (2)$$

Where ν is the Poisson's ratio of soil

Both the elastic shear (G_{max}) and bulk (B) modulus of the layers were considered to be varying with depth from ground surface (being the function of confining pressure). As bulk modulus of soil increases during dynamic simulation due to decrease in the voids ratio of soil, therefore an average value of bulk modulus was calculated by taking average value of Poisson's ratio as 0.3 and 0.35 for medium dense and dense layers, respectively.

The plastic and hydraulic properties of the soil layers such as drained peak friction angle and permeability determined with the help of the consolidated drained triaxial test and constant head permeability tests respectively, were taken from literature [12]. As the shear-volume coupling relationship is already given in the pore pressure formulation with the Finn/Byrne model, therefore the dilation angle which also defines the same relationship was taken as zero.

This model was calibrated with the constant volume simple shear tests for both types of samples [13]. A number of strain-controlled cyclic simple shear tests were conducted at the Nottingham Centre for Geomechanics laboratory. The element strain-controlled cyclic constant volume simple shear test was simulated as a single element in FLAC 2D dynamic using this liquefaction constitutive model as shown in Fig. 3.

The formulation in Finn/Byrne liquefaction model, based on the coupling between shear strain and volumetric strain, is represented by the following equation proposed by Byrne [13].

$$\Delta\varepsilon_v = C_1\left(\frac{C_2\varepsilon_v}{\gamma}\right) \tag{3}$$

$\Delta\varepsilon_v$ is the increment in volumetric strain that occurs in each cycle, ε_v is the accumulated volumetric strain for previous cycle, γ is the shear strain amplitude for the current cycle, C_1 and C_2 are constants dependent on the volumetric strain.

The initial input values of the Finn/Byrne constitutive model parameters (C_1 and C_2) were estimated from the following formula, developed by Byrne [14].

$$C_1 = 7600(D_r)^{-2.5} \tag{4}$$

$$C_2 = \frac{0.4}{C_1} \tag{5}$$

Where D_r is relative density of sand.

The initial value of the reference strain constant (γ_{ref}) for the Hardin-Drnevich hysteretic dynamic damping model (the value that matches with modulus reduction and damping ratio increase curves given by Seed and Idriss [10] for typical sand) was taken as 0.05, as suggested in the FLAC manual [9].

Then, a trial and error method was used to arrive at the final best values of the Finn/Byrne model parameters (C_1 and C_2) and the Hardin-Drnevich hysteretic dynamic damping model reference strain constant (γ_{ref}) constant.

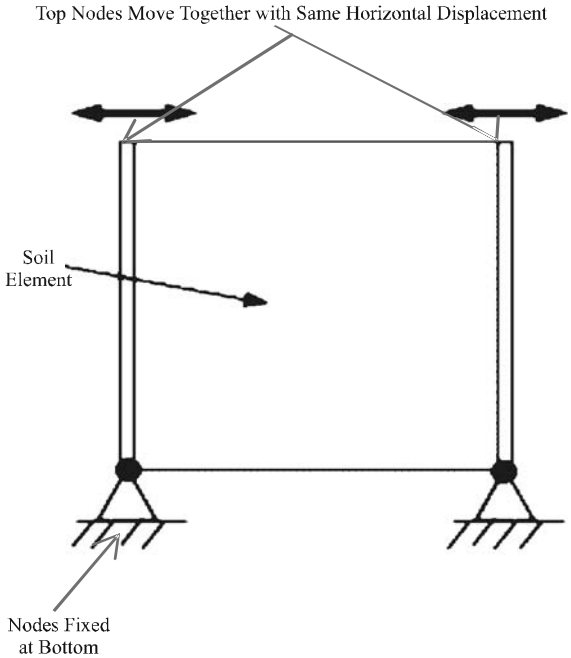

FIG. 3. FLAC SINGLE ELEMENT CYCLIC SIMPLE SHEAR TEST

This (trial and error) was achieved by performing a number of FLAC simulations of the test with varying values of the parameters and the best fit to the experimental results was obtained. The average values of the parameters based on the three tests to be used for the FLAC modelling and analysis are shown in Table 2.

2.6 Soil Constitutive Model Calibration

The above mentioned constitutive model was calibrated with the constant volume simple shear tests for medium dense samples at three strain amplitudes 1, 2 and 5%.

Figs. 4-5 present the predicted and measured stress-strain and pore pressure development behaviour with FLAC 2D simulation of the test and the laboratory element test for medium dense samples. The results for stress-strain behaviour and the pore pressure of the numerical simulation using the Finn/Byrne model combined with the Hardin-Drnevich dynamic hysteretic damping model predicts a reasonable representation of the laboratory experimental tests. However, the shear stress in the initial cycles is slightly different than that measured in laboratory tests.

2.7 Dynamic Soil Damping

As stated earlier, Hardin-Drnevich hysteretic damping model was combined with Mohr-Coulomb based Finn/ Byrne constitutive model for modelling soil behaviour in liquefaction. This combined constitutive model also provides the hysteric damping for dissipation of the energy of an earthquake waves. With this combined model, during the dynamic simulation in the elastic range of soil, the damping ratio increases with the strain level when the soil is deformed. In the plastic range, when the soil reaches the state of plastic flow, further simulation is continued with only the Finn/Byrne plasticity soil model to avoid unrealistic overdamping of the deposit when the plastic model provided adequate damping in the plasticity range of the soil (as suggested in the FLAC dynamic manual [9]. In addition to hysteretic damping prescribed by the constitutive model, a nominal Rayleigh damping proportional to the system stiffness and mass matrix was provided with a nominal damping ratio of 0.5% as suggested in the FLAC Manual [9]. The Rayleigh damping with an average 5% damping ratio (with all modes of vibration) was applied to the structure [11-12].

TABLE 2. PARAMETERS FOR SOIL MODEL USED FOR FLAC MODELLING

Model Parameters	Medium Dense Sand Layer	Dense Sand Layer
C_1	1.2	0.43
C_2	0.33	3.75
γ_{ref}	0.05	0.05

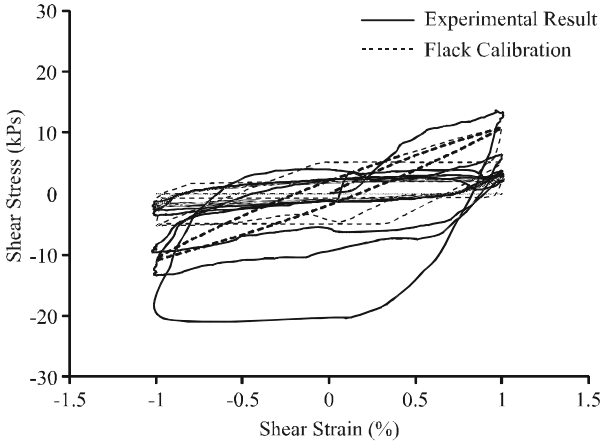

FIG. 4. FLAC CALIBRATION OF STRESS-STRAIN BEHAVIOUR

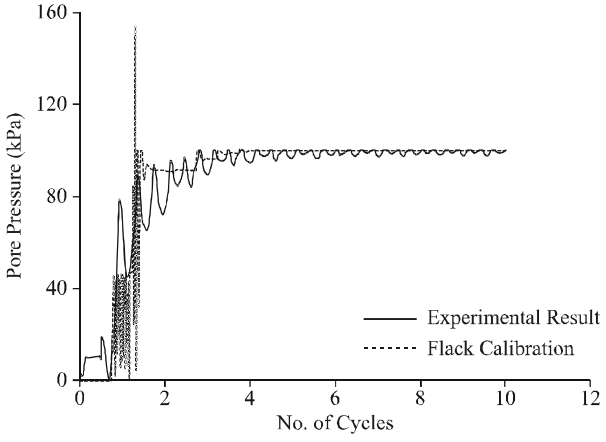

FIG. 5. FLAC CALIBRATION OF PORE PRESSURE

2.8 Earthquake Motion

In order to obtain consistent trends from the sensitivity analysis, a standard sinusoidal velocity wave was applied as a design earthquake at the base of the model with the velocity amplitude of 0.2 m/sec, which represents an extreme earthquake event with a ground acceleration of 0.35g (approximately 3.5 m/sec^2). This corresponds with the ultimate limit state of collapse of the structures in liquefaction. A frequency of 3.0Hz was used and the wave was applied for duration of 10 seconds. These figures are the common figures recorded during an earthquake. The wave was applied at the base of the model in horizontal direction for the FLAC 2D model. The simulation was continued for a few seconds after stopping the wave after 10 seconds to allow the model to come into equilibrium. Further, the vertical component of motion was not applied to allow the observed behaviour to tie with the effect of horizontal component of motion. The vertical component was separately taken in one study to see its effects on the performance.

2.9 FLAC 2D Model Development

A two dimensional rectangular uniform zone size mesh as shown in Fig. 6 ,was developed for this analysis. The mesh consisted of four node quadrilateral elements, with every node in the mesh connected to four other nodes, with the exception of nodes at the boundaries of the mesh. In the finite difference method like any other numerical method the accuracy of the results depends upon the grids used to represent the physical system.

In order to keep a balance between accuracy of results (making the mesh as fine as possible and keeping the aspect ratio to 1) and simulation time, three uniform meshes of zone size 0.5 x0.5, 0.25x0.25 and 0.125x0.125m were tested. The results showed that there was no significant difference in the response of soil-structure system during simulation with all three meshes, particularly in the settlement of the structures which is the key variable in this study, with all the three sizes of mesh. FLAC 2D simulation time of finer mesh of 0.25x0.25m zone size was as long as 60 hrs as compared to the reasonable time of 6 hrs for courser mesh of 0.5x0.5m zone size. In the view of the numerical testing results, uniform mesh of 0.5x0.5m zone size with aspect ratio of exactly 1 was selected for this study.

The boundaries of the model are located in such a way that the responses of the structure soil-structure system (stresses, strains and pore pressure) in the area of interest are not affected. To achieve this purpose, the boundaries of the grid were located at a distance of 5 and 3 times the soil deposit thickness on each side of centre of structure. To further check the effect of boundaries they were located at a distance of 2.5 times the thickness from each side of centre of structure. The results showed that the response was not significantly affected when boundaries were located 2.5 times from the centre of structure pad. Finally, the model with boundaries 3 times the deposit thickness (60m each side of centre of footing) was selected.

For the static equilibrium analysis of the model, before dynamic analysis, fixed lateral and bottom boundaries were applied. For dynamic analysis, free field boundaries were

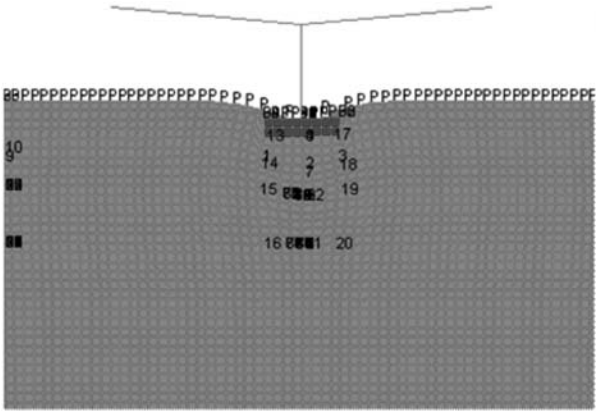

FIG. 6. THE SETTLEMENT OF THE FOOTING AND THE STRUCTURE

applied along two lateral boundaries of the model. With free field boundaries, displacements to the left of boundary is forced to be equal the displacement right of boundaries in free field [9] to representing free field condition away from the influence of structure. For hydraulic boundaries, the pore pressures along the top boundary of model were fixed at zero values to represent a free drainage top surface, whereas lateral and bottom boundaries were taken as impervious.

2.10 Static Equilibrium

The static elastic-perfectly plastic analysis was carried out with the Mohr-Coulomb constitutive model before the dynamic analysis to distribute the initial stresses and pore pressures in the model and to bring the soil deposit and structure into equilibrium after the construction of the structure. The initial stresses and pore pressures in the soil deposit were assigned as linearly varying with depth from ground surface before the static analysis (Table 3).

3. RESULTS AND DISCUSSION

In order to understand the mechanism of liquefaction-related large permanent deformations of the soil-structure system during the earthquake in a 2D environment, the isolated shallow strip plane strain footing pad 4m wide and 1m thick, supporting a typical simple frame structure, was founded on the ground at the depth of 1m from the level ground surface as shown in Fig. 6.

TABLE 3. INDEX PROPERTIES OF LEIGHTON BUZZARD E-FRACTION SAND

Properties	Values
Mean Grain Size D50: mm	0.142
Specific Gravity, G_s	2.65
e_{max}	1.025
e_{min}	0.65

The history of the settlements at the top of the centre of the footing pad as presented in Fig. 7 show that the settlement is 86cm (or vertical displacement of -86cm) of the footing pad at 7.5 seconds of cyclic excitation. The simulation stopped at 7.5 seconds of dynamic time due to large shear deformations in the foundation soil when the soil liquefied beneath and around footing pad. The footing pad and the supported column rotate by 3cm about the centre of the pad during the cyclic loading.

These large vertical movements (settlements) of footing were triggered initially at a higher rate just after a half cycle of cyclic loading and continue to increase at a relatively lower constant rate until the end of cyclic excitation under the structural load when the soil reached the softened or liquefaction state. The rotation of the footing was triggered due to the horizontal inertial force during cyclic excitation. This trend of settlement of shallow footing was also observed by other researchers [6-7,15] in centrifuge tests.

The contours of vertical displacement after the dynamic event as presented in Fig. 8, show that the rigid block, comprising of footing pad and a nearly triangular wedge of soil beneath it, vertically displace in punching shear in the foundation soil. As a result of this shear punching of the rigid block, the soil beneath the footing pad displaces

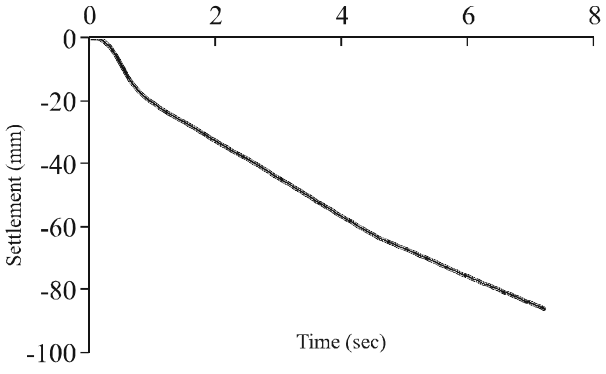

FIG. 7. THE SETTLEMENT OF FOOTING VERSUS TIME

to the depth of about 8 m in the relatively shallow zone. The soil adjacent to the edge of the footing pad displaces in the narrow area of about 0.5m adjacent to edge of the pad with large vertical displacements. The area around the pad at shallow level near the ground surface shows the bulging of soil.

The contours of horizontal displacement as presented in Fig. 9 show that when the rigid block comprising footing and wedge of soil punches vertically, it displaces the soil in horizontal direction in the wide zone of nearly 10m around each edge of the footing pad. Larger movements occur near the edge of the footing which decreases with distance from it. The movements also vary with depth with maximum values at the depth of about 3m from footing base.

This type of bearing capacity failure (shear failure) can be classified as Terzaghi's punching type shear failure which is normally encountered in very soft soil due to the liquefaction. In this type of shear failure, shallow depth of foundation soil beneath and narrow area (width) around the footing is involved in shearing because the liquefied soft material is not capable to transfer loads to wider and deeper area around the footing due to its low shear stiffness.

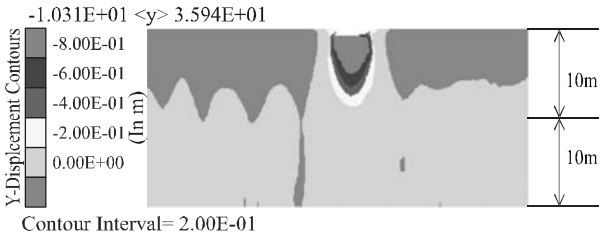

FIG. 8. CONTOURS OF VERTICAL DISPLACEMENT

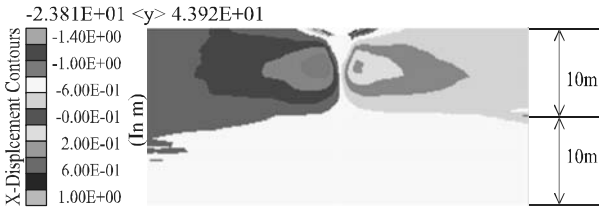

FIG. 9. CONTOURS OF HORIZONTAL DISPLACEMENT

The history of the pore pressure immediately under the centre of the footing pad as presented in Fig. 10 show that excess pore pressure rises from the initial hydrostatic to the peak value of 58 kPa in the initial few cycles of cyclic loading which soon reverse back from the peak value of 58-13 kPa because of the effect of dilation (expansion) at large static shear strains caused by monotonic shearing under the load of structure. Again the excess pore pressure gradually and slightly rises from 13 kPa to bit higher value of 28 kPa and remain at this level in the later cycles of cyclic excitation. These trends of excess pore pressure rising in just few cycles and then soon dropping due to dilation were also observed in centrifuge tests [16].

Due to the rise in excess pore pressure to the peak, the effective stress in the soil as presented in Fig. 11, decreases from the initial effective stress of 83.5 kPa to lower value of 30 kPa at the time corresponding to peak pore pressure in the initial cycles. The effective stress again increases to the higher value of 70 kPa when the pore pressures drops due to the effect of dilation under the influence of structure. Then, effective stress remains

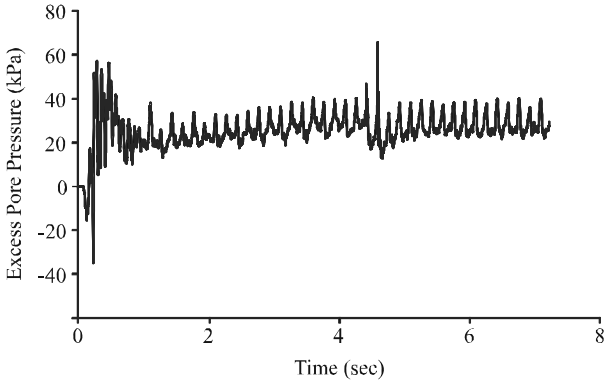

FIG. 10. PORE PRESSURE VERSUS TIME IMMEDIATELY UNDER THE CENTRE OF FOOTING

at around this relatively higher value during the later cycles of loading. Due to the decrease of effective stress in the initial cycles when the pore pressure is at the peak, shear stiffness and strength of the soil decreases, which triggers liquefaction-related large shear deformations and settlements at constant volume (undrained) condition of soil under the load of structure. When the pore pressure drops due to the effects of dilation, the effective stress of the soil again increases and the soil regains most of its stiffness in shear in the later cycles. As a result the rate of liquefaction-related shear deformations and settlements at constant volume condition should have diminished in the later cycles. However, a relatively high rate of settlements until the end of cyclic loading may not be due to shear deformations at constant volume (undrained) conditions.

The history of pore pressure in the free field away from the influence of structure at the same depth as immediately under the structure as presented in Fig. 12 show that excess pore pressure rises from initial hydrostatic to the peak of 13 kPa in the initial cycles of cyclic loading which remain constantly high in the later cycles of dynamic loading. This trend of pore pressure rise and then constantly high in free field was also observed in centrifuge [7].

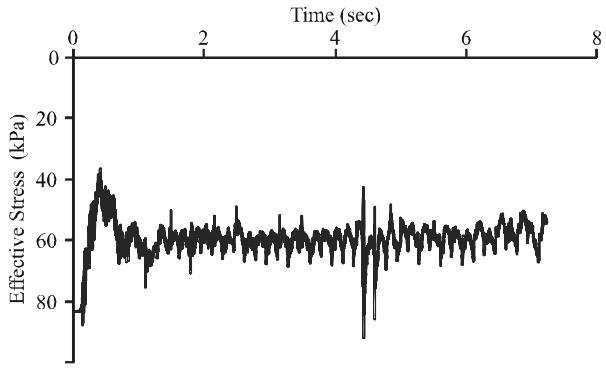

FIG. 11. EFFECTIVE STRESS VERSUS TIME UNDER THE CENTRE OF FOOTING

Due to this rise in pore pressure, the effective stress as presented in Fig. 13 decreases from the initial value of 9.8 kPa to the very low value of 2 kPa. Due to this loss of effective stress to very low values, shear stiffness and strength of soil is almost lost resulting in complete softening and liquefaction of soil in the free field.

The history of pore pressure at the level of 4m depth under the centre of the footing pad as presented in Fig. 14 shows that the excess pore pressure rise from the initial hydrostatic to the peak of 82 kPa in the initial cycles of cyclic loading. The excess pore pressure soon drops to 42 kPa because of the effect of dilation (expansion) due to larger shear strains by monotonic shearing under the influence of the structure. The excess pore pressure remains relatively high at 42 kPa in the

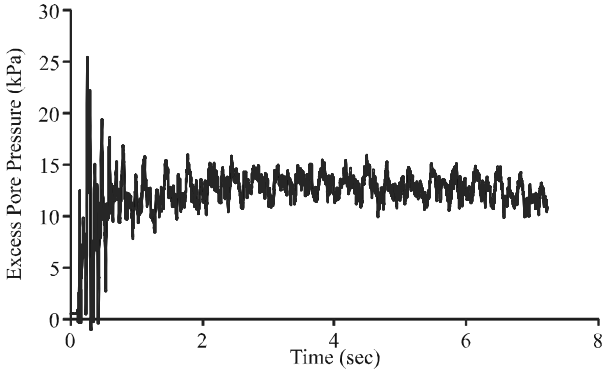

FIG. 12. PORE PRESSURE VERSUS TIME IN THE FREE FIELD AT SHALLOW DEPTH

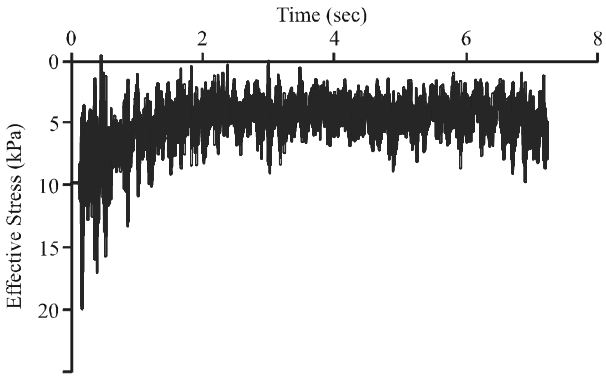

FIG. 13. EFFECTIVE STRESS VERSUS TIME IN FREE FIELD AT SHALLOW DEPTH

later cycles of cyclic excitation at this deep level from footing base.

Due to the rise in pore pressure to the peak, the effective stress as shown in Fig. 15 decreases from initial effective stress of 95.5-30 kPa in the initial cycles of cycling loading which soon increases to the constantly higher value of 80 kPa when the pore pressure decreases due to effects of dilation of soil. The soil regains most of its stiffness and strength in the later cycles as effective stress again increases.

The history of pore pressure in the free field away from the influence of structure at the same depth of 4m as that under the structure as presented in Fig.16 shows that the excess pore pressure increase from the initial hydrostatic to the peak of 47 kPa in the initial cycles of cyclic loading and remain constantly high in the later cycles of cyclic loading.

Due to this rise in pore pressure, effective stress as shown in Fig. 17 decreases from its initial value of 38 kPa to a very low value of 10 kPa which remains constantly low in the later cycles of cyclic excitation. Due this lose of effective stress, shear strength and stiffness of soil is completely lost in the free field in the same way as seen at shallow depth.

These results suggest that the behaviour of foundation soil under the footing of structure is relatively stiffer as

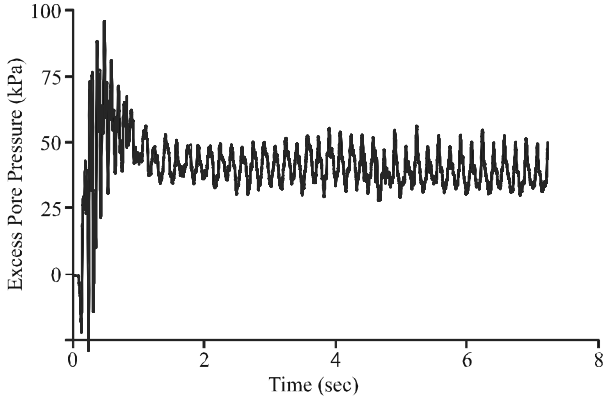

FIG. 14. PORE PRESSURE VERSUS TIME UNDER STRUCTURE AT DEPTH OF 4m

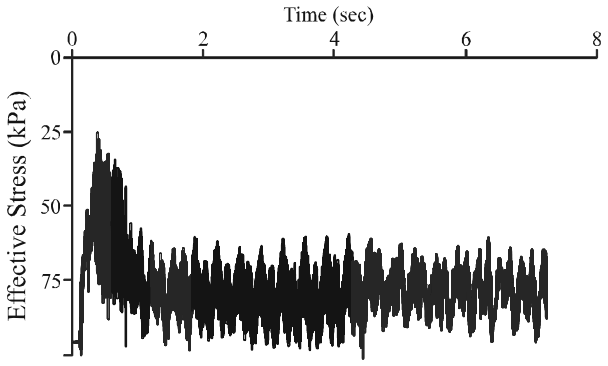

FIG. 15. EFFECTIVE STRESS VERSUS TIME UNDER STRUCTURE AT 4m DEPTH

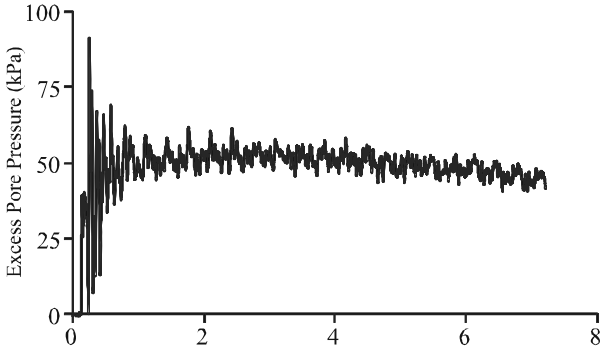

FIG. 16. PORE PRESSURE VERSUS TIME IN FREE FIELD AT THE DEPTH OF 4m

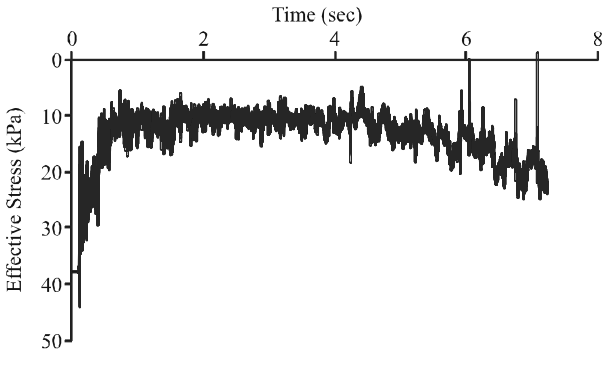

FIG. 17. EFFECTIVE STRESS VERSUS TIME IN THE FREE FIELD AT THE DEPTH OF 4m

compared to the free field due to the high initial effective stress under load of structure. Further, under the structure, pore pressure soon drops because of the effect of dilation of soil due to monotonic shearing of the soil under the load of structure. Due to this beneficial effect of dilation, effective stress increases again which results in the increase in shear strength and stiffness of soil under the footing. These results also indicate that though under the influence of structure soil may not as much liquefy or become soft as in the free field, the pore pressure still rises to the high levels at which significant softening occurs under the footing in foundation soil, which triggers liquefaction-related large settlements in initial cycles of loading as shear deformation of soil occurs at constant volume condition. At the deeper level of 4m from the footing base under the structure, same effects of confinement from structure and the dilation were seen but at this deeper level these effects are relatively less pronounced as compared to a shallower depth. In the free field, the soil remains in a liquefied and softened state throughout the history of cyclic loading at all depths.

The contours of shear strains as presented in Fig. 18 also show punching type shear failure of footing during liquefaction in which, the rigid block comprising footing and nearly triangular wedge of soil behaving as a rigid body, punches in shear in soft ground which causes shearing of the soil in very narrow and shallow zones of soil around the footing pad.

The histories of shear strains under the centre of the footing pad at the depth of 4m from the footing base as presented in Fig. 19 show that shear strains increase at a higher rate in the initial cycles of cyclic loading when the shear stiffness of soil starts to decrease due to the development of high pore pressure and the decrease of effective stress. These shear strains or deformations continue in the later cycles, though at a relatively lower constant rate until the end of cyclic excitation because of relatively higher (excess) pore pressure throughout the cyclic history. Very large shear strains (24%) are predicted at the end of cyclic excitation due to monotonic shearing under influence of structure load. Due to this large monotonic shearing under the structure which causes dilation of soil, the pore pressure under the structure soon drops after rise in the initial cycles.

The histories of shear strain in the free field at the same depth of 4m as under the structure presented in Fig. 20 indicate that, shear strain is as low as 1% without the influence of structure load. Though this shear strain is low, still it is two orders higher than the threshold value of 0.01%, as mentioned by Dorby, et. al. [17] that causes the development of pore pressure to high value and nearly complete loss of effective stress, shear strength and stiffness of soil in free field as seen previously.

FIG. 18. SHEAR STRAIN CONTOURS UNDER THE FOOTING PAD

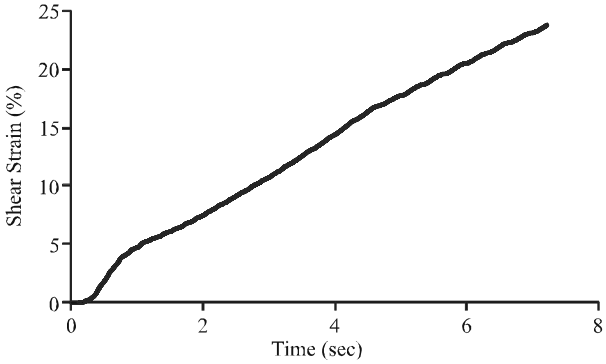

FIG. 19. SHEAR STRAIN VERSUS TIME UNDER THE CENTRE OF FOOTING

The histories of volumetric strain or volume change (compression) under the centre of the footing pad as presented in Fig. 21 show that the volumetric strains increase at a lower rate in the initial cycles of cyclic loading mainly due to air voids compression in soil and at a relatively higher rate in the later cycles once dissipation of the pore pressures is started in later cycles when the steady state of flow of the water to the top drainage surface is established. The large volumetric strains or volume changes during cyclic loading are due to the fast development of pore pressure as a result of cyclic shear straining which pushes the water towards the top drainage surface .This fast dissipation of pore pressure during cyclic loading causes rapid volume changes. These rapid volume changes during cyclic loading were also reported by Dashti, et. al. [6] in centrifuge tests.

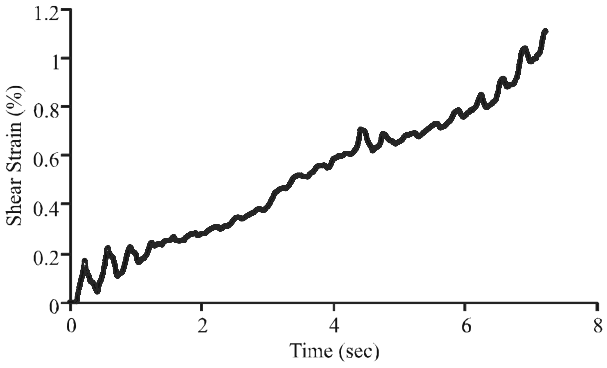

FIG. 20. SHEAR STRAIN VERSUS TIME IN THE FREE FIELD

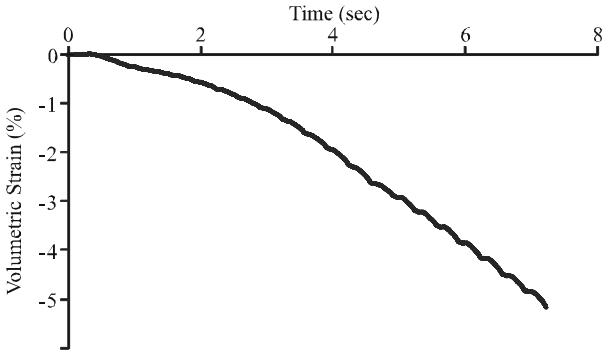

FIG. 21. VOLUMETRIC STRAIN VERSUS TIME UNDER THE CENTRE OF FOOTING

The histories of shear and volumetric strains under the centre of the footing pad suggest that large settlements of footing in the initial cycles of cyclic loading are mainly triggered due to large shear deformations at nearly constant volume conditions when soil reaches the liquefied state. The settlements of the footing in the later cycles of cyclic loading are mainly due to the rapid volume change or reconsolidation of soil due to the fast pore pressure dissipation during cyclic loading. During the cyclic loading excess pore pressures are developed and dissipated at high rate due to cyclic shearing of soil and flow of water to the top drainage free surface. Although, liquefaction related shear deformations and settlements at constant volume condition (due to excess pore pressure and loss of effective stress) continue throughout the history of cyclic excitation, their rate is higher in the initial cycles.

The comparison of the velocity history at the base of the footing as presented in Fig. 22, with the history at the base of the model as presented in Fig. 23, shows that the amplitude of velocity at the centre of the base of the footing is 0.15 m/sec as against the input value of 0.2 m/sec at the base of the model in the first cycle of cyclic excitation. This amplitude of velocity decreases to as low as 0.02 m/sec (10% of base velocity) due to partial decoupling of the footing pad and structure from the foundation soil when the soil losses its stiffness due to high pore pressure and reach the liquefied state in the initial cycles of cyclic loading. In the later cycles, the amplitude of velocity starts to increase to around 0.13 m/sec (around half of input amplitude at the base of model) when the pore pressure under the footing decrease due to the effect of dilation and soil regain stiffness.

The above results suggest that at the moment when the soil reached a liquefied state, the transmission of amplitude

of motion from the bedrock to the structure through the soil deposit significantly reduced and the footing remained partially decoupled from foundation soil. This attenuation in velocity of the footing during liquefaction of soil was also reported by others in centrifuge tests [6-7].

The histories of rotation of footing as shown in Fig. 24 shows that footing continue to rotate to 3cm about the centre as the cyclic velocity is acting during excitation. This rotation of footing in the cyclic loading is due to large shear deformations at nearly constant volume conditions when soil the liquefies.

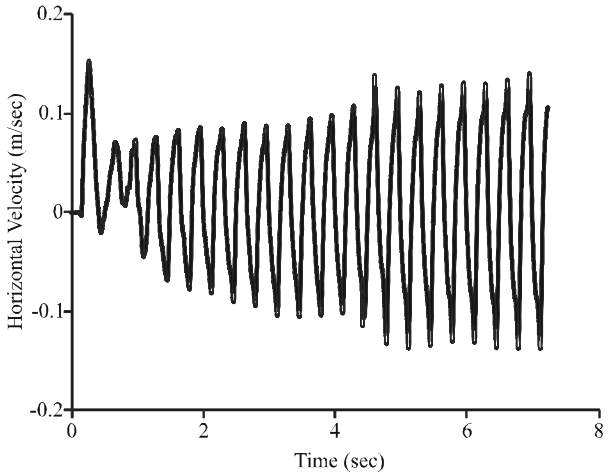

FIG. 22. HORIZONTAL VELOCITY AT THE BASE OF FOOTING VERSUS TIME

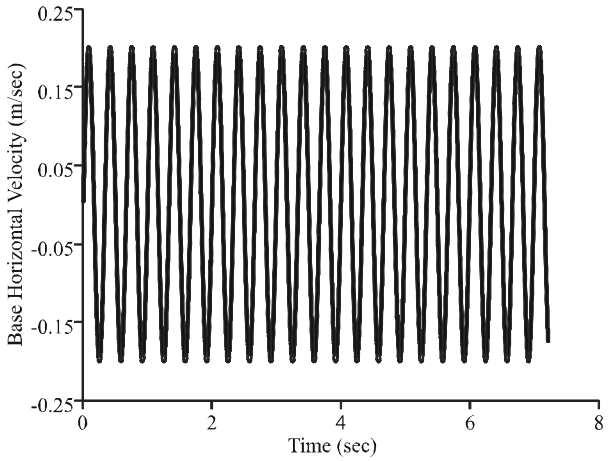

FIG. 23. INPUT HORIZONTAL VELOCITY AT THE BASE OF MODEL VERSUS TIME

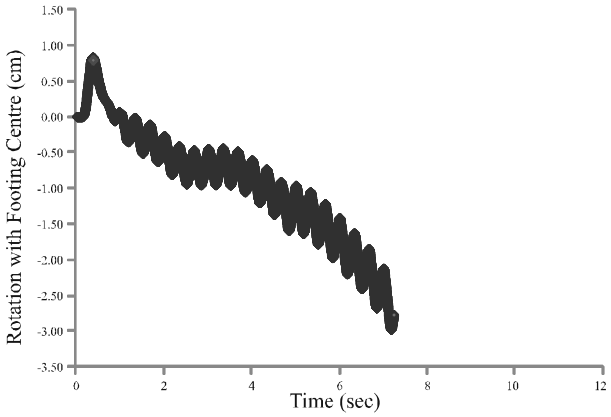

FIG. 24. ROTATION OF FOOTING WITH CENTRE VERSUS TIME

4. CONCLUSIONS

The following conclusions can be drawn for the case analysed in the test conditions.

(i) A shallow footing settles by 86cm and rotates by 3cm about the centre of the pad in punching type bearing capacity (shear) failures when the foundation soil liquefies.

(ii) Excess pore pressure under the footing quickly rise to the peak levels in a few cycles but soon reverses back to lower levels due to the effects of dilation caused by monotonic shearing from structural load. In the free field pore pressure reaches peak values in a few cycles and remains constantly high in later cycles. Due to the rise of pore pressure, soil completely liquefies in the free field but under the structure the behaviour of soil is relatively stiffer.

The large settlements of footing in the initial cycles of cyclic loading are mainly triggered due to large shear deformations at nearly constant volume conditions when soil reaches the liquefied state. The settlements of the footing in the later cycles of cyclic loading are mainly

due to the rapid volume change or reconsolidation of soil due to the fast pore pressure dissipation during cyclic loading.

(i) Motions (velocities) transmitted to the structure decrease as pore pressure rises when the soil is in a softened state. At this softened state, the footing is nearly decoupled from the base motion. This indicates that due to this softening smaller motions are transmitted to the footing during liquefaction.

(ii) These static shear deformation and lateral movement of soil under the structure are two important phenomena of liquefaction-related large settlements of shallow foundations of structure.

ACKNOWLEDGEMENTS

The research presented in this paper was carried out as part of Ph.D. (First Author) studies at University of Nottingham, UK. The authors wish to acknowledge the support received from University of Nottingham, and Mehran University of Engineering & Technology, Jamshoro, Pakistan. In addition, the authors wish to acknowledge the excellent technical support received from the staff of the Nottingham Centre for Geomechanics, UK.

REFERENCES

[1] Kishida, H., "Damage to Reinforced Concrete Buildings in Niigata City with Special Reference to Foundation Engineering", Soils and Foundations, Vololume 6, No. 1, pp. 71-88, Japan, 1966.

[2] Ohsaki, Y., "Niigata Earthquake, Building Damage and Soil Condition", Soils and Foundations, Volume 3, No. 2, pp. 14-37, Japan, 1964.

[3] Seed, H. B., and Idriss, I.M., "Analysis of Soil Liquefaction, Niigata Earthquake", Journal of Soil Mechanics and Foundation Engineering Division, ASCE, Volume 93, No. 3, pp. 83-108, USA, 1967.

[4] Yoshimi, Y., and Tokimatsu, K., "Settlement of Buildings on Saturated Soils During Earthquakes", Soils and Foundations, Volume 17, No. 1, pp. 23-38, Japan, 1977.

[5] Martin, J.R., Olgun, C.G., Mitchell, J.K., and Durgunoglu, H.T., "High Modulus Columns for Liquefaction Mitigation", Journal of Geotechnical and Geoenvironmental Engineering, ASCE, Volume 130, No. 6, pp. 561-571, USA, 2004.

[6] Dashti, S., Bray, J.D., Pestana, J.M., Riemer, M.R., and Wilson, D., "Mechanisms of Seismically-Induced Settlement of Buildings with Shallow Foundations on Liquefiable Soil", Journal of Geotechnical Geoenvironmental Engineering, Volume 136, No. 1, pp. 151-164. ASCE, USA, 2010.

[7] Coelho, P.A.L.F., Haigh, S.K., and Madabhushi, S.P.G., "Post-Earthquake Behaviour of Footings Employing Densification to Mitigate Liquefaction", Ground Improvement, Volume 1, No. 1, pp. 45-53, UK, 2007.

[8] Simon, N.E., and Menzies, B.K., "A Short Course in Foundation Engineering", IPC Science and Technology Press, UK, 1975.

[9] Itasca FLAC2D V6.0/FLAC3D V3.1: "Fast Lagrangian Analysis of Continua", User Manuals, Itasca Consulting Group, Inc., Minneapoli ,USA, 2009.

[10] Seed, H.B., and Idriss, I.M., "Soil Moduli and Damping Factors for Dynamic Response Analyses", Report EERC 70-10, Earthquake Engineering Research Centre, University of California, Berkeley, CA, USA, 1970.

[11] Hardin, B.O., Drnevich, V.P., "Shear Modulus and Damping in Soils: Design Equations and Curves", Journal of the Soil Mechanics and Foundations Division, ASCE, Volume 98, No. 7, pp. 667-692, USA, 1972.

[12] Coelho, P.A.L.F., "In Situ Densification as Liquefaction Mitigation Measure", Ph.D. Thesis, University of Cambridge, UK, 2007.

[13] Almani, Z.A., Memon, A.A., and Memon, N.A., “Effects of the Length of Jet Grouted Columns and Soil Profile on the Settlement of Shallow Foundations”, Mehran University Research Journal of Engineering & Technology, Volume 31, No. 3, pp. 517-528, Jamshoro, Pakistan, July, 2012.

[14] Byrne, P.M. , "A Cyclic Shear-Volume Coupling and Pore Pressure Model for Sand", Proceeding of Second International Conference on Recent Advances in Geotechnical Earthquake Engineering and Soil Dynamics, Volume 1, University of Missouri, Rolla, Missouri, pp. 47-55, USA, 1991.

[15] Clough, R., and Penzien J, "Dynamics of Structures", Second Edition, McGraw Hill, Inc.,USA, 1993.

[16] Chopra, A.K, “Dynamics of Structures”, 2th Edition, Prentice Hall International, USA, 2000.

[17] Dobry, R., Ladd, R.S., Yokel, R.Y., and Chung, R.M., "Prediction of Pore Water Pressure Build-Up and Liquefaction of Sands During Earthquakes by Cyclic Strain Method", NBS Building Science Series 138, Washington DC, USA, 1982.